ISO-DOSE MAP GENERATION AND DOSE-AREA PRODUCT CALCULATION THROUGH DIGITAL IMAGE PROCESSING OF SCANNED IRRADIATED RADIOCHROMIC FILMS

GENERACIÓN DE MAPAS DE ISO-DOSIS Y CÁLCULO DEL PRODUCTO DOSIS-ÁREA USANDO PROCESAMIENTO DIGITAL DE IMÁGENES EN PELÍCULAS RADIOCRÓMICAS IRRADIADAS Y ESCANEADAS

Y. Ruiz-Gonzalez[a†], S. Rodríguez-Ledesma[b], J.E. Paz Viera[c], J.V. Lorenzo Ginori[a]

a) Centro de Investigaciones de la Informática, Universidad Central "Marta Abreu" de Las Villas, Santa Clara, Cuba; yuselyr@uclv.edu.cu[†]
b) Centro de Ingeniería Clínica y Electromedicina, Santa Clara, Cuba.
c) Zimmer Biomet, Toronto, Canada.
† corresponding author

Iso-dose maps creation and kerma-area products calculation are important procedures in radiotherapy and medical imaging. In this work, a method is presented to obtain iso-dose maps through digital processing of the images obtained from radiochromic films, which are employed to estimate the dose absorbed by the patient. The kerma-area product in selected regions of interest (ROIs) in the iso-dose map was then evaluated. The images were obtained by scanning the irradiated films using a commercial flatbed scanner. The iso-dose areas were extracted by means of an image segmentation algorithm, while calibration for a particular film to obtain a sensitometric curve relating dose to film darkening, was also made. A software interface allowed introducing the scanned image for the estimation of kerma-area products by defining the ROI interactively. The methods developed in this work allowed to implement a software application to obtain the iso-dose maps and kerma-area product in selected ROIs.

La creación de mapas de isodosis y el cálculo subsiguiente del producto kerma-área son procedimientos importantes en radioterapia e imagenología médica. En este trabajo se presenta un método para obtener mapas de isodosis a través del procesamiento digital de imágenes de las películas radiocrómicas utilizadas para estimar las dosis absorbidas por los pacientes en estos procedimientos. También se evalúa el producto kerma-área en regiones de interés (ROI) seleccionadas en los mapas de isodosis. Las imágenes se obtuvieron escaneando las películas irradiadas utilizando un escáner plano comercial. Las áreas de isodosis se extrajeron mediante un algoritmo de segmentación, además se realizó la calibración utilizando una película en particular, para obtener una curva sensitométrica que relaciona la dosis con el oscurecimiento de la película. Una interfaz de software unifica los métodos desarrollados y permite procesar imágenes escaneadas para la estimación de productos dosis–área definiendo las ROI de forma interactiva.

I. INTRODUCTION

The measurement of ionizing radiation has evolved progressively over the last decades with the introduction of new methods as well as new detectors. Among the latest, radiochromic films have gained attention due to their suitable properties for the task of measuring the absorbed dose. Some of these properties are: accuracy, precision, operational dose range, good response to dose in terms of changes in film darkness, spatial resolution, near tissue-equivalence absorption properties, and ease of handling. Such properties make these materials closer to the ideal dosimeters and ahead of other methods and materials [1, 2]. Additionally radiochromic films do not require any special developmental procedure so they can give a permanent absolute value of the absolute dose at any time when they are preserved correctly. Radiochromic media for dosimetry can be found also in various forms including liquid solutions, gels, waveguides and films. Recent examples of current applications of radiochromic films which include applications outside the

medical field can be found in [2–5]. A radiochromic film has the special feature of altering its coloration according to the radiation dose absorbed, which is - related to its internal composition. A typical film contains an active layer in its interior made of an opacifying agent. This layer is protected by other external layers such as two polyester protecting layers in the most external positions which enclose an adhesive surface and the active layer [6, 7].

Upon irradiation, a polymerization process is initiated in the polyacetylenic compound resulting in the immediate change in the color of the coating. The color darkens in proportion to the radiation exposure [1, 6]. The reduction in light passing through the film is a measure of its 'blackness' or optical density (OD). This metric can be calculated as follows:

$$\text{OD} = \frac{1}{4} \log_{10}\left(\frac{I_0}{I}\right), \tag{1}$$

where I_0 is the light intensity with no film present and I is the light intensity after passing through the film. Note

that since $\left(\frac{I_0}{T}\right)$ has an exponential relationship to the dose, the OD is appropriately linear with dose. The acceptance of this relationship has led to the wide use of the film as a dosimeter [1].
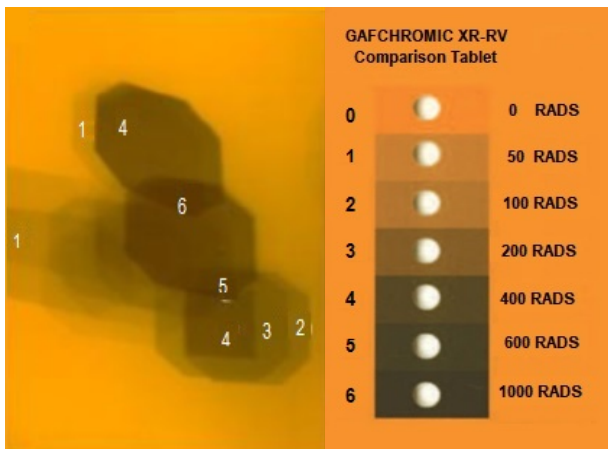

Figure 1. Scanned image of an irradiated film showing the labels of the differently irradiated zones.

Fig. 1 shows the scanned image of an irradiated film and a comparison strip which usually accompanies the film pack when it is purchased. It is used to have an estimate of radiation dose by visually comparing the opacity of the film with the strip specific values. This way, the precision of estimated values is affected by quantization as well as by the subjective evaluation of the observer.

Usually the film is placed between the radiation source and the object to be irradiated. Then, the degree of darkening can be measured by employing apparatus such as reflection or transmission densitometers, spectrophotometers, scanners and opto-electronic instrumentation [8,9].

It is a regular practice to neglect small uncertainties such as the overall uncertainty of the dose measurement in the reference field, the uncertainty due to the non-uniform thickness of the film sensitive layer, and uncertainties associated with the equipment used to measure OD. Then, if the films are correctly calibrated, they can operate as absolute dosimeters yielding information directly about absorbed dose in absorbed radiation measurement units (Gy) [1,2,10].

Radiochromic films have been used in therapy [3, 11] as well as in diagnostic or treatment [12], to have an estimate of the absorbed dose by the patient subjected to any of these procedures. In this case, the film is placed between the radiation source and the patient, covering the area to be irradiated and remaining in that position until the procedure is done. No further procedure is required with the film (such as development or other chemical treatment) to estimate the degree of opacity caused by the absorbed radiation.

Previous dosimeters such as semiconductors or TLDs, usually mounted in ensembles, while offering precise measurements in certain locations, also offered a lower spatial resolution. With the introduction of radiochromic films, an accurate value of absorbed dose can be estimated at any point within the area covered by the film. Since the film darkens in proportion to

radiation exposure, it is possible to measure the darkening and use it as a means for determining the amount of radiation exposure. In this way, the film may be employed not only as a radiation dosimeter but also to map radiation fields [1].

Previous works have measured film opacity employing the calibration strip to perform statistical analysis of irradiation procedures [6]. However, in the last years there has been an increase of methods for estimating absorbed dose from the films by employing apparatus such as densitometers, or more advanced methods such as automatically estimating absorbed dose from processing digital images of the scanned irradiated films [11–14].

Making use of appropriate Digital Image Processing algorithms, this work aims at the automatic segmentation of iso–dose areas in digital images from scanned irradiated films. In order to accomplish this, the way to obtain a two-dimensional (2D) OD fluence map is to be developed, which in turn can be converted to a 2D dose map. Segmenting the 2D map in areas whose dose is constrained to some interval in order to allow differentiating areas in the film that were irradiated in a similar amount, was the previous step in order to build the corresponding iso-dose map. This map has the purpose of facilitating the task (for the specialist) of easily locating these areas in order to measure the received patient radiation dose. This could be accomplished by simply pointing at them using computer software with an adequate visualization system. Another objective is the calculation from the iso-dose map of the kerma-area product for polygonal areas defined interactively.

II. MATERIALS AND METHODS

II.1. *General aspects of the calibrating procedure*

Film calibration is a process that yields a relationship between absorbed dose and film opacity. It is the first step before any other procedure is realized with the film in order to obtain any value of absorbed dose within the film's operation range from its opacity degree. Film opacity can be measured either by employing transmission or reflection densitometers, spectrophotometers, and/or flatbed scanners. In the case of scanners the acquired images should be stored in lossless compression file formats such as TIFF or BMP in order to maintain the highest quality of image representation avoiding the effects of lossy compression [15]. The curve obtained is called the sensitometric curve and is a characteristic of the film employed(in these experiments (GAFCHROMIC XR-RV2 film [16,17]). This film usually comes in a landscape format of 14 (height) $\times$ 17 (wide) inches. In order to characterize the film, a group of small pieces of size 3×4 cm were sectioned from it maintaining the same landscape direction. The manufacturer specifies that GAFCHROMIC XR-RV2 could be used within the range 0.02 Gy to 50 Gy, with an energetic dependence less than 8 %, and between 30 keV and 30 MeV. In this case to the effect of selecting an appropriate method for interpolation, the range of radiation doses used in the samples was extended up to 100 Gy. It is known that the manufacturer recommends the use of the film in the range 0.02-50 Gy, however it is also

known that the human visual system is capable to discern only up to 30 intensity levels in an image. This means that in the comparisons table of Fig. 1, the darkest samples look very similar and the naked human eye could not discern clearly darker regions. This is not the case with digital images having intensities represented by 8 bit pixels: the computer could discern 256 intensity levels and it is possible to consider the hypothesis that with the method used in this work the useful irradiation dose range could be extended beyond 50 Gy. With the purpose of obtaining a preliminary clue about the ability of the method used here to discern high irradiation levels beyond the recommended range for the radiochromic film used in this application, as well as selecting an appropriate interpolation method capable of working properly in these conditions, here the range was extended up to 100 Gy as can be appreciated in the samples shown in Fig. 2, samples 14-16.

The protocol designed for the manipulation of the films (and the film pieces during calibration) pre- during-, and post-irradiation was established according to previous reviews [1, 18]. In the conducted experiments the OD estimation of irradiated film (and/or of the film segments) was carried out employing the conventional flatbed scanner HP ScanJet 3500c. All calculations were done employing MatLab [19].

II.2. Film calibration

As a first step, a group of 16 film pieces of size 3×4 cm were cut off out of the radiochromic film in order to irradiate them at different doses, and then, to measure film opacity at this values to obtain the curve relating OD with the absorbed dose. The dose values were: 125, 250, 375, 500, 750, 1000, 1500, 2000, 2500, 3000, 3500, 4000, 5000, 6500, 8000 and 10000 mGy. Irradiation took place at Departamento de Energía Nuclear (DEN), UFPE, Brasil, using a Pantak industrial X-Ray equipment, bipolar model, series 2HF420, with energies RQR6 ($V = 80$ kV, $I = 10$ mA, and beam quality of 3.01 mmAl of CSR) and RQR8 ($V = 100$ kV, $I = 10$ mA, and beam quality of 3.97 mmAl of CSR) [14]. An envelope was built in order to hold the pieces together within an irradiation area of 15 cm diameter at 100 cm distance to the source.

Twenty four hours after all pieces were irradiated, the OD was measured employing scanner HP Scanjet 3500c and digital image processing algorithms. Fig. 2 shows the scanned images of a set of irradiated film pieces.

The analysis of film opacity could be done using separately the intensity corresponding to any of the three RGB color components (Red, Green and Blue) or their combination in the Visual channel instead, obtained by means of the relation:

$$V = 0.299 I_R + 0.587 I_G + 0.114 I_B,$$
$$V = 0.299 R + 0.587 G + 0.114 B, \qquad (2)$$

where I_R, I_G, and I_B are the pixel intensities in the Red, Green and Blue channels respectively [16]. However, it has been demonstrated in previous works [16, 20] that the intensity of the red component is more sensitive to radiation

in radiochromic films. Having this in mind, the OD was calculated from the red channel pixel intensities in the scanned images according to the relation:

$$OD_{net} = OD_i - OD_n = \log\left(\frac{I_n - I_b}{I_i - I_b}\right), \qquad (3)$$

where OD_i and OD_n are the ODs of irradiated and non-irradiated films respectively, I_b is the background pixel value obtained while scanning a black surface and I_i and I_n are the pixel values in irradiated and non-irradiated images respectively using the red component. This process does not depend upon the file format used to save the images.
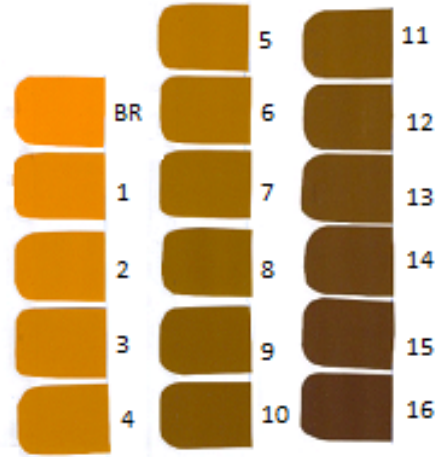

Figure 2. The sixteen irradiated pieces (1 to 16) of GAFCHROMIC XR-RV2 film, plus the non-irradiated piece (BR) at energy RQR6. The film sections and their respective doses are as follow: 1-125, 2-250, 3-375, 4-500, 5-750, 6-1000, 7-1500, 8-2000, 9-2500, 10-3000, 11-3500, 12-4000, 13-5000, 14-6500, 15-8000 and 16-10000 mGy.

To the effects of image processing, calibration curves were calculated to allow determining the dose corresponding to the specific irradiation in a film point, expressed in terms of the intensity's complement in the digital image. Here, if the intensities of the digital images from the pieces are represented in a scale such that $0 \le I \le 1$, the intensity's complement $C_i = 1 - I$ is an indicator of the film darkness that holds a bi-univocal relationship with the image intensity and with OD_{net} in equation (3) thus allowing determining a direct relationship between dose and intensity. The values of irradiation corresponding to every value of intensity can be obtained by interpolating the ordered intensity-irradiation pairs corresponding to the above-mentioned sixteen irradiated film pieces.

II.3. Determining the Ci-dose curves through interpolation

In order to determine the dose corresponding to any point in the image of the scanned radiochromic film, the curves C_i-dose are to be determined from the experimental values calculated for the sixteen irradiated pieces previously mentioned, using interpolation techniques.

Conventional polynomial and cubic splines were the interpolation methods implemented and tested in order

to select the one that provides the best results. For polynomial interpolation, a continuous polynomial function Φ determined from the 16 experimental points should be capable of predicting the dose value from C_i for all the other values inside and near to the interval extended from lowest to highest dose. Here is an example for a given polynomial of order n,

$$C_i = \Phi(x; a_0, \ldots, a_n) = a_0 + a_1 x + a_2 x^2 + \ldots + a_n x^n, \qquad (4)$$

where C_i is the intensity's complement and x is the dose (D). Polynomials of degrees 3, 4 and 5 were used to obtain the curves and compare their effectiveness.

Cubic splines use third order polynomials for a piecewise interpolation between the experimental points, with the constraint that the first and second derivatives of the curves must have the same value at both sides of the initial points. Notice that with this method the interpolated curve is forced to pass across the experimental data points.

Decimation was used to compare the interpolation methods. In this case, one out of two and one out of three were chosen to determine the polynomial coefficients or the coefficients for the cubic splines. Then, the ordinate values at the remaining points were compared to the value predicted by the interpolated curve at the respective abscissas and the root mean squared (rms) errors were compared statistically by means of the Wilcoxon signed rank test [21]. In this case the null hypothesis was that the mean rms error was the same for the given pair of methods ($\mu_1 = \mu_2$, against the alternative hypothesis that one of the methods is better than the other $\mu_1 \neq \mu_2$, with $p = 0.05$. Once the interpolation method to be used was determined, it was actually used to obtain interpolated values of D from the C_i values of the pixels in the film, using the corresponding function characterized by their sets of coefficients.

II.4. Obtaining the iso-dose map

Once the C_i-dose curves were obtained, a continuous dose map was created in which the intensity of each pixel in the scanned radiochromic film was substituted by its corresponding dose value. Then, the map was median filtered to eliminate possible outliers and afterwards segmented in areas for which the dose values pertain to a prescribed interval. The intervals used for this segmentation are shown in Table 1.

Binary images were obtained by thresholding the intensity image at the pre-defined levels and assigning the value 1 to the region with a dose higher than the threshold. Then, a binary image associated to the corresponding iso-dose region was obtained by the set intersection $A \cap B^C$, where A and B are regions that correspond to contiguous threshold levels (where threshold in A is lower than that in B), as shown in Fig. 3 together with the general intensity histogram.

Each connected component (region) associated to the corresponding dose interval in the image was then labeled with a capital letter, as indicated in Table 1. In the image to be shown in the graphical interface, positioning the letters for this labeling was not a trivial task, as these letters should appear as centered as possible in each region. In order to accomplish this, the maximum of the distance transform in a binary image in which the logical value 0 was assigned to the region of interest and a logical 1 to the background, was used to determine the most centered points. The distance transform [22] of a binary image is defined as follows: for every pixel x in set A, $DT(A)$ is its distance from x to the complement of A,

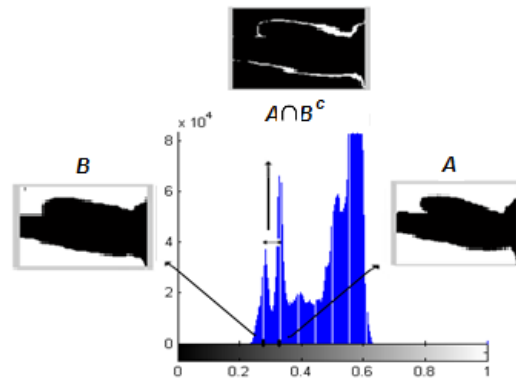$$DT(A)(x) = min\left\{d(x, y), \ y \in A^C\right\}. \qquad (5)$$

Figure 3. Binary images A and B obtained by thresholding the intensity image at the levels indicated in the histogram, and the difference image obtained through A∩B^C.

Table 1. Iso-dose intervals and identifying characters.

Label	Lower dose	Higher dose
A	0	150
B	150	250
C	250	500
D	500	750
E	750	1000
F	1000	1500
G	1500	1750
H	1750	2000
I	2000	2250
J	2250	2500
K	2500	3000
L	3000	3500
M	3500	4000
N	4000	4500
O	4500	5000
P	5000	Inf

From the definition of the distance transform it is clear that $DT(A)$ will exhibit at least one maxima at the farthest point from the region borders. In case that more than one maximum exist, one of them is selected for placement of the character that will identify the corresponding iso-dose region. Then, a binary image is created with a 'one' in each of the $DT(A)$ maximum points and zero level in the rest of the image. These characters were built by morphological dilation of the binary

points with a binary image of the character that identifies the region (see Table 1). Fig. 4 shows the various steps in labeling one iso-dose region from the distance map calculation, where each labeled iso-dose region is to be distinguished by its color according to an appropriate color map.

II.5. Calculation of the kerma-area products.

Calculation of the kerma-area product in a user-defined region can be easily accomplished once the continuous dose map was obtained. In order to perform this calculation, it is necessary to know the area covered by one pixel in the image. Let R be the selected region, d_i the dose associated to the i-th pixel p_i within this region and A_p the radiochromic film area associated to an individual pixel in the image. Then, the kerma-area product can be obtained as:

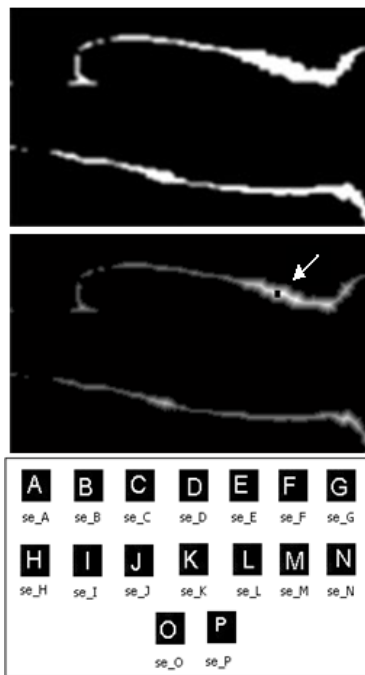$$DAP = A_p \sum_{p_i \in R} \lim d_i. \tag{6}$$

Figure 4. Labeling an iso-dose region, from top to bottom: binary map of the iso-dose region, distance map showing a maximum (most centered) pixel, small black square pointed by an arrow, and binary letters used as structuring elements for morphological dilation.

II.6. The software for film image analysis

The software algorithm created to obtain the iso-dose maps and kerma-area calculations was structured in two operation modes: calibration and measurement. In the calibration mode, the dose values corresponding to the irradiated radiochromic film pieces and the scanned images of the pieces are introduced as data. Then, the C_i-dose curve is obtained by interpolation and shown graphically.

In the measurement mode, the image of a radiochromic film to be evaluated is loaded, and the pixel area is also introduced. Here the pixel area depends upon both

the scanner resolution employed and the actual film size. Segmentation by thresholding is performed to obtain the iso-dose areas. These are labeled by means of morphological operations as was explained before. Finally, a polygonal region where the iso-dose area is to be evaluated is defined interactively by the user and the corresponding kerma-area product is calculated.

III. RESULTS AND DISCUSSION

In this work, the complementary intensity versus irradiation dose curves were used and two interpolation methods were tested: polynomial and splines. In the case of polynomial interpolation it was found experimentally that order 4 provided the best results and it was used in the comparison to splines, which is shown in Table 2 for an experiment with an irradiation dose interval from 0 to 5000 mGy. Fig. 5 shows the interpolated curves corresponding to these two methods. It is apparent that for the data used to obtain these curves, the fact that splines force the interpolated curve to pass across the experimental points determined the presence of a larger rms error using this method. It was found also that when the experimental points are measured carefully this difference was not statistically significant when subjected to the Wilcoxon signed rank test.
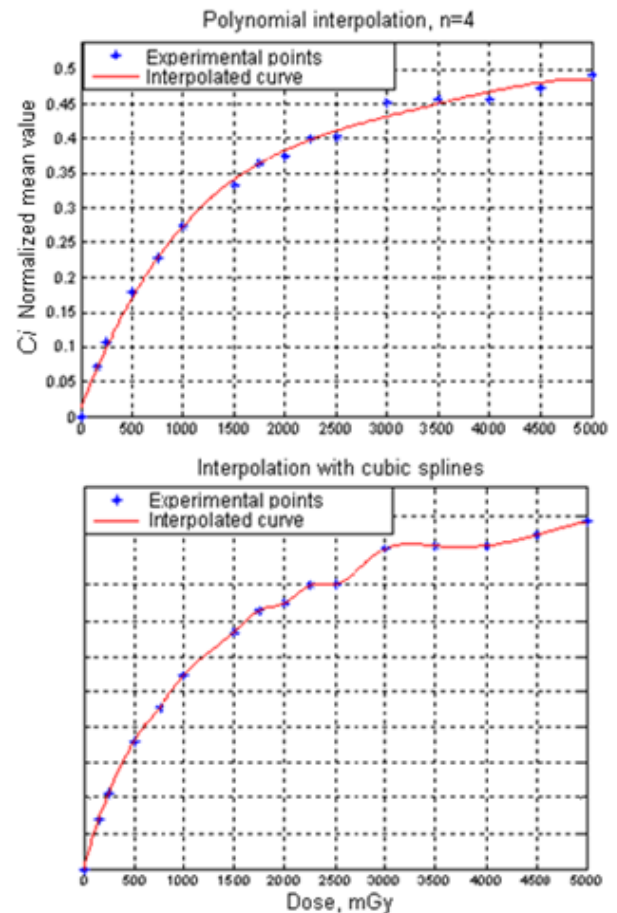

Figure 5. Comparison of interpolation by polynomial fitting and cubic splines.

Table 2. Errors in the interpolation methods. A: Predicting 8 samples from the remaining 8 (decimating by 2), B Predicting 10 samples from the remaining 6 (decimating by 3).

	Polynomial 4th order	Cubic splines
A	0.0715	0.2077
B	0.1056	0.1314

However, when using a wider irradiation range up to 10000 mGy, this situation changes because the polynomial fitting tends to exhibit some degree of oscillation in the range of high values. This determined that in a statistical evaluation using again the Wilcoxon signed rank test for this entire interval, the spline interpolation exhibited a better result than the polynomial one. This determined the use of splines as the method of choice (see Fig. 6). Notice also that the points obtained for the highest irradiation values suggest that the radiochromic film might discern and estimate radiation doses beyond 5000 mGy when using digital image processing techniques, a result that should be confirmed with more formal experiments.
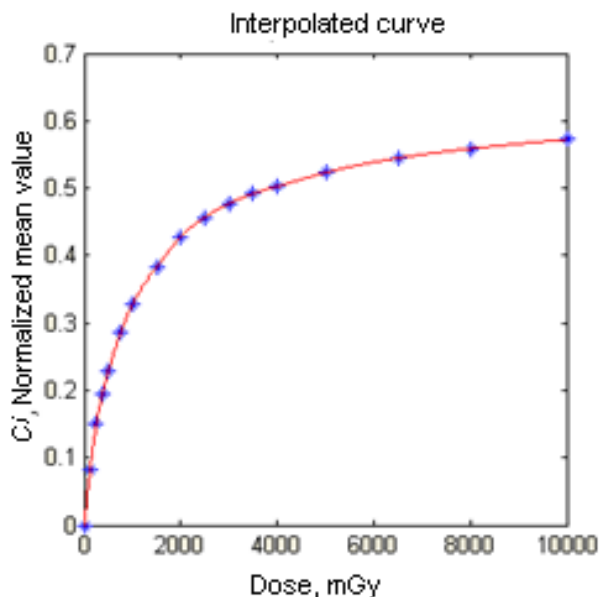

Figure 6. Interpolation with splines for the entire range up to 10000 mGy.

Iso-dose maps can be obtained in low computation time, even considering that the morphological procedures used for labeling tend to increase the computational load. Fig. 7 shows a typical iso-dose map and Table 3 shows the computation time for the processing of a specific radiochromic film, including that corresponding to the interpolation phase. For these measurements, an implementation in Matlab 7.0 was executed in a computer with an Intel Quad-Core processor at 2.33 MHz and with 2 GB RAM.

Table 3. Computer time for some of the main processes.

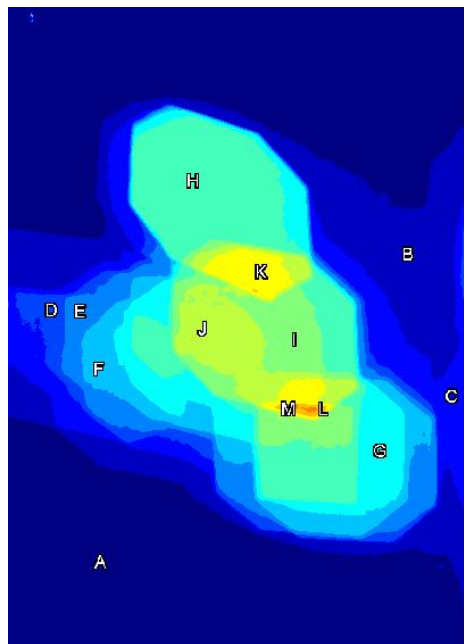| Program function	Time (seconds)
Polynomial Interpolation	0.93
Spline interpolation	0.92
Iso-dose map	21.32
kerma-area product	0.033

Figure 7. An example of labeled iso-dose map.

IV. CONCLUSION

A complete software system devoted to the creation of iso-dose maps from images of irradiated radiochromic films scanned in a conventional flatbed scanner has been presented in this paper. Special attention was devoted to find the best interpolation method to construct a complementary intensity-dose curve that allowed calculating the dose corresponding to a pixel with some value of intensity in the digital image produced by the scanner. It was found that there was not a statistically significant difference between polynomial and spline interpolation up to 5000 mGy while splines showed a better performance in the range up to 10000 mGy, which can be attributed to the effects of oscillation in the polynomials.

To conclude, a method to segment the film image into iso-dose regions using thresholds, and labeling these regions by means of morphological image processing, was introduced and demonstrated. This would allow differentiating areas in the film that were irradiated in a similar amount. The system would facilitate the specialists to easily locate these areas in order to measure the radiation dose received by the patient. Kerma-area products for an interactively defined polygonal area can also be calculated easily from the iso-dose map obtained. The computer time consumption of the developed software is low, allowing an efficient application of the system.

V. REFERENCES

[1] S. Devic, N. Tomic, and D. Lewis, Physica Medica **32**, 4, (2016).

[2] Y. Tiantan, L.H. Luthjens, A. Gasparini and J.M. Warman, Rad. Phys. Chem. **133**, 37 (2017).

[3] S. Devic, L. LiHeng, N. Tomic, H. Bekerat, M. Morcos, M. Popovic, P. Watson, S. Aldelaijan and J. Seuntjens, Physica Medica **64**, 40 (2019).

[4] R. Holla et al., J. Med Phys. **44**(3), 145 (2019).

[5] R. Yan, J. Yun, J. Gurtler, and X. Fan, Postharvest Biol. and Technol. **127**, 14 (2017).

[6] S. Devic, Physica Medica **27**, 3 (2011).

[7] H.-Y. Shih, D. Lewis, and J. Anyumba, EP1430310A4, (2014).

[8] J. M. Lárraga-Gutiérrez, O. A. García-Garduño, C. Treviño-Palacios, and J. A. Herrera-González, Phys. Medica Eur. J. Med. Phys. **47**, (2018).

[9] P. Casolaro, et al. Scientific Reports Open **9**(5307), 1 (2019).

[10] S. Devic, et al., Med. Phys. **32**, 7 (2005).

[11] M. C. Battaglia, "Dosimetry studies for radiation therapy with photons and radiobiology using low-energy protons", PhD Thesis, Universidad de Sevilla, España, 2017.

[12] A. Neocleous, E. Yakoumakis, G. Gialousis, A. Dimitriadis, N. Yakoumakis, and E. Georgiou, Radiat. Prot. Dosimetry **147**, 1 (2011).

[13] W. V. Segura, Tecnol. **33**, 1 (2020).

[14] M.E. Howard, M.G. Herman, M.P. Grams, PLoS ONE **15**(5), e0233562 (2020).

[15] R. C. Gonzalez and R. E. Wood, Digital Image Processing Using Matlab, (GP, New Delhi, 2009).

[16] A. I. Mendoza-Moctezuma et al., AIP Conference Proceedings **1310**, 1 (2010).

[17] R. Sánchez, E. Vano, J. M. Fernández, A. Machado, and N. Roas, Radiat. Prot. Dosimetry **147**, 1 (2011).

[18] A. Niroomand-Rad, *et al.*, Med. Phys. **25**, 11 (1998).

[19] "MATLAB Documentation" (https://www.mathworks.com/help/matlab/).

[20] N. Lunelli, M. S. Rochas, J. E. Paz-Viera, and H. J. Khoury, in V Latin American Congress on Biomedical Engineering CLAIB 2011 edited by J. F. Folgueras et al.(Springer, IFMBE proceedings, 2013).

[21] F. Wilcoxon, Biom. Bull. **1**, 6 (1945).

[22] P. Soille, Morphological Image Analysis - Principles and Applications, (Germany, Springer Verlag, 2003).